 MCB, vol.3, no.2, pp.69-77, 2006

Three-Dimensional Molecular Phase Separation and Flow Patterns with Novel Multilevel Fluidics

Jui-Ming Yang* **and Philip R. LeDuc*,†**

Abstract: Inorganic and organic integrated systems detect, process, and respond to signals from solid media. Advances in fluidic systems have offered an alternative to traditional signaling methods through the development of aqueous signaling systems. Here, we show an experimentally simple mechanically governed fluidic system that creates three-dimensional molecular multiphase separation in a combination of discrete and continuous gradients analogous to digital and analog signals that can be used for controlled spatiotemporal cellular stimulation. We accomplish the pattern formation by fabricating a compartmentalized multi-level fluidics device where a network of capillaries converges into a main channel. Simultaneous control of the fluid streams in the horizontal and vertical planes allows us to create hybrid aqueous patterns. This soft lithography system enables controlled diffusion schemes within the laminar flow regime in three dimensions and overcomes the limitations of monophasic delivery and planar constraints. Our fluidic device has potential applications in a wide range of systems from three-dimensional biological control in cell structure and motility studies to fluidic computational devices.

1 Introduction

The evolution of mechanically-based fluidic systems has recently led to the hypothesizing and pursuit of novel scientific questions in diverse areas ranging from computational logic to subcellular stimulation (1-3). However, advances in answering these questions impose new challenges for developing integrated fluidic capacities using lithographic methods. Through the increase in the sophistication of microfluidic systems, researchers have pursued alternative methods to produce integrated processes including logic operations, fluidic control, and detection on the chip (4,5). Although these processes can be controlled through an electronic framework, unconventional media may provide distinct advantages which would have applications in computational, decision making, or environmental control. For example, streams in the microfluidic domain have been used to create a chemical stream being present or absent under two-dimensional control (6). The ability to have precision beyond solely binary on-off signals into three dimensions would provide significant advantages on multiple fronts. To build these fluidic devices, fabrication techniques as practiced in the electronic and microelectromechanical fields are utilized (7-9) where micrometer scale components are fabricated on silicon wafers (10-13). Microchannels, which are made from fabrication and inverted molding processes (14-16) have been used in a multitude of diverse applications including optical lattice sorting (17,18), memory and control devices (1, 19-21), and colloidal assembly methods (22-25). However, due to the lithographic techniques used, a major limitation is that the devices are often two-dimensional in nature. Thus, the ability to have spatial distribution in three dimensions is constrained. In addition, specific systems have been developed with three-dimensional characteristics in their final device arrangement yet the fluid distribution in these is limited to the predefined three-dimensional architectural configuration of the fabricated structures (26-29). In this study we design and fabricate our mechanically-governed **Mu**ltiphase **F**luidics **S**eparation in **3** **D**imensions (MuFS-3D) device and demonstrate the active manipulation and delivery of aqueous phases not only in the horizontal direction but in the vertical one as well. This device can be applied to cellular mechanics as the ability for cells to move, deform, and respond to forces is directly related to the chemical environment in which cells reside. Through being able to manipulate local domains of a single cell in three-dimensions, we can alter the internal environment of the cell, which helps to bridge the gap between molecular and cellular response; this gap is separated by a ten-thousand times size difference. One example of our sys-

* Departments of Mechanical and Biomedical Engineering, and Biological Sciences, Carnegie Mellon University, 5000 Forbes Avenue, Pittsburgh, Pennsylvania 15213

† Corresponding Author, prleduc@cmu.edu

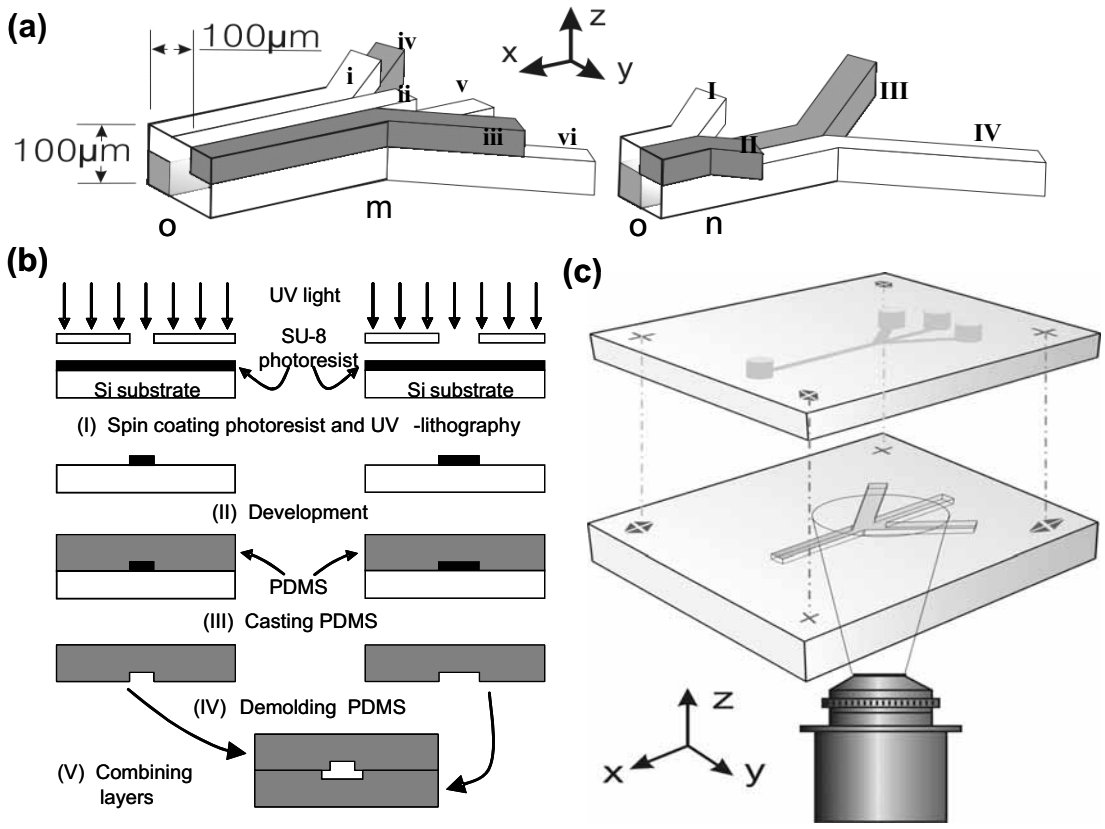

Figure 1 : The Multiphase Fluidics Separation 3D (MuFS-3D) device. (a) Schematics of 6-inlet and 4-inlet systems. In the 4-inlet system, the intersection point of the inlets in the upper and lower layers was shifted in the x-axis (vertically-offset). In the 6-inlet device, the main channel of both upper and lower layers aligned completely above each other (vertically-aligned). Grey channels represent the presence of fluorescent molecules. White channels represent the absence of fluorescent molecules. The various inlets in the 6-inlet system are labelled i – vi and those in the 4-inlet device are labelled I – IV. Location *m* (for vertically-aligned devices) and location *n* (in vertically-offset systems) denote the intersection point where the various inlets converge into the main channel. Location *o* refers to a distance further away (along the x-axis) from the intersection point. The distance separating locations *m* and *o* was approximately 3 cm and the distance between locations *n* and *o* was approximately 1 cm. (b) Schematics for the MuFS-3D fabrication process. SU-8 photoresist (black box) was spun onto a silicon wafer (Si substrate) and thermally cured. A transparent mask (white box) with the features printed on it was placed on top of the SU-8 photoresist and exposed to ultraviolet (UV) light (I). The resulting pattern was then chemically reacted to create the reverse features of the fluidic channels, i.e., the mold (II). Polydimethylsiloxane (PDMS; grey box) was poured onto the mold and thermally cured (III). Each PDMS slab was then peeled off of the mold to create the fluidic channels (IV). One PDMS slab was then inverted, aligned, and sealed on top of a second PDMS slab (V). (c) Schematic of vertical and horizontal alignment for epi-fluorescent and confocal microscope visualization. The x-y-z axes indicate the orientation throughout the figures.

tem affecting mechanics is through locally modifying the cell structure (i.e. cytoskeleton), which would directly affect the response of the cell to mechanics as the dominate factor in cells is their biochemical regulation. Furthermore, by altering the viscosity in the adjacent lanes, this device would allow a force gradient to be applied through control of shear stress. This new fluidic system provides a significant advance in the ability to create patterns of molecules and emulates digital and analog signals integrated within three-dimensional domains; this is essential in cellular and molecular research.

2 Methods

Channels were fabricated on silicon wafers by pattern transferring of SU-8 photoresist (Microchem), which were then used to create microfluidic channel molds (Fig. 1a and 1b). Polydimethylsiloxane (PDMS) was cast against these molds and placed against another PDMS layer; the channels were sealed to #1 borosilicate glass coverslides for microscopic visualization. Plasma oxidation of the PDMS was utilized to strengthen this surface adhesion. Our MuFS-3D system was built through the alignment of two PDMS layers, which was accomplished under light microscopy. The substrate and the PDMS slabs were first cleaned with tape to prepare the bonding surface. Due to the natural adhesion of the PDMS surfaces during contact, the surfaces of the two slabs were treated with a thin layer of water at a localized region of the bonding surface to form an intermediate layer and make relative movement between the layers possible. This additional step prevented the hydrophobic surfaces from self-annealing during alignment. Once aligned, the two slabs were placed under vacuum and bonded. Both the substrate and PDMS slabs were placed in the oxygen plasma chamber with a controlled voltage and duration (100 V, 30$\sim$60 sec.). The area with the water layer was not bonded, but this did not affect our device because this location was far from the channel area.

Three-dimensional multiphase flows were generated by stacking PDMS slabs which combined microchannels in the horizontal and vertical planes (Fig. 1a). Each PDMS slab has embedded predesigned features, where the main channel was 100 μm in width and 50 μm in height. The combination of PDMS slabs with different patterns resulted in the 6-inlet and 4-inlet MuFS-3D devices shown in Figure 1a. In our 6-inlet device, the main channel of both upper and lower layers were completely aligned (vertically-aligned); whereas in the 4-inlet system, the intersection point of the inlets in the upper and lower layers were shifted with respect to the x-axis (vertically-offset). Throughout this study, the various inlets in the 4-inlet device are labelled I – IV and those in the 6-inlet system are labelled i – vi (Fig. 1a).

Cascade blue, texas red and fluorescein were used to distinguish spatiotemporal distribution of fluorescent streams in our MuFS-3D devices. In addition, phosphate buffered saline (PBS) alone was used as the non-fluorescent control. After streaming various solutions through the physically separated inlet channels we observed parallel flow streams that converged into the main channel where the selective separation of the dyes was maintained. The lack of fluid mixing was dictated by the Reynolds number, Re = $\nu d\rho/\mu$ (velocity v, diameter of the channel d, density of the liquid ρ, and viscosity μ), which is a dimensionless ratio of inertial forces to viscous forces. This formula predicted the tendency of a flowing fluid to develop laminar or turbulent flow. When Re was approximately less than 1000, fluid mixing was inhibited and laminar flow was maintained (30); in our system, Re was below 1. We controlled the three-dimensional chemical delivery with respect to the laminar flow behavior through leveraging this laminar flow behavior. To accomplish this, one level of fluidic delivery was supplemented with an adjacent fabricated slab above the base slab (Fig. 1c). For the fabrication, the channel resolution is limited by the mask and pattern transfer. For our application, we do not require dimensions smaller than tens of micrometers; this is easily achieved by conventional soft lithography. The thickness of the PDMS slabs is limited by the focal depth of the microscope objective as there are adjacent layers of PDMS. In our experiments, we were limited to 2 micrometers. We introduced distinct solutions into the systems and the different phases of fluid flowing from both vertically and horizontally separated inlets converged into the main channel. Cascade blue, texas red and fluorescein (Molecular Probes) were diluted in PBS to a working concentration of 100 μg/ml. These three dyes were visualized using DAPI, tetramethyl rhodamine isothiocyanate, and fluorescein isothiocyanate filter sets, respectively. Fluorescence was visualized under 10, 20, 40 or 100X objectives of an epi-fluorescence Zeiss Axiovert microscope or an Olympus Fluoroview BX61 confocal microscope. Digital images were captured and processed using National Institute of Health Image. Images for the multilevel devices generally were constrained to the 40X, 1.0 numerical objective due to the working distance necessary for capturing images at multiple heights. For visualizing the streams, the resolution ideally is the same in the vertical and horizontal directions, but the ability to visualize it is limited by the microscope; optical microscopy resolution is theoretically limited by approximately half of the width of the excitation wavelength.

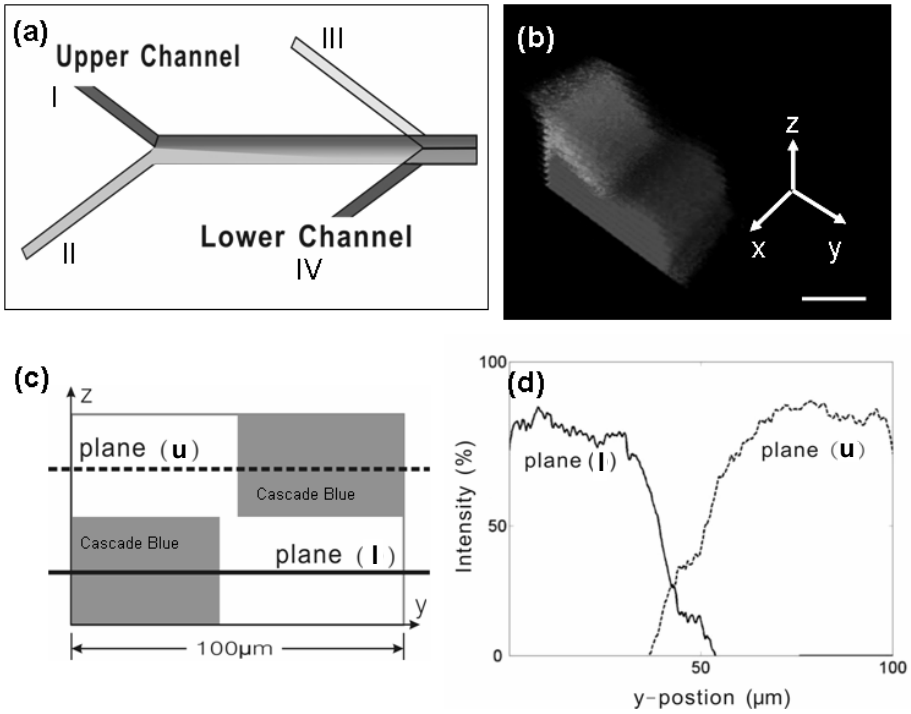

Figure 2 : Complex three-dimensional pattern formation through delivery of molecular solutions into the main channel. (a) Schematic of fluidic organization and (b) confocal microscope image of a section of the 4-inlet vertically-offset MuFS-3D device at location *n*. Fluorescein was added into inlet I, texas red into inlet IV, and PBS into inlets II and III. Scale bar = 30 μm. (c) Three dimensional pattern formation using a 6-inlet vertically-aligned MuFS-3D system. Cascade blue was added into inlets iii and iv and Phosphate Buffered Saline (PBS) into inlets i, ii, v and vi. Slices at specific x-y planes were observed. Cross-section **u** represents the molecular distribution in the upper layer whereas cross-section **l** indicates the distribution in the lower layer. (d) Normalized intensity plot of a sloping gradient profile at location *o*. For all three schematics, cascade blue is represented as the grey area whereas the white sections indicate the location for PBS.

3 Results and Discussion

Complex delivery of solutions into the main channel was analyzed by confocal microscopy in the 4-inlet vertically-offset MuFS-3D device at location *n*. The result of controlling the chemical distribution of the aqueous solutions was to create three-dimensional hybrid patterns shown by the schematic in Figure 2a. Fluorescein was added into inlet I, texas red was added into inlet IV, and PBS into inlets II and III. The three-dimensional confocal reconstruction of the section analyzed is shown in Figure 2b. Fluorescein was observed in the upper left and texas red in the bottom right quadrants (corresponding to inlets I and IV, respectively). These patterns with the MUFS-3D were created through the mechanisms of: 1) three-dimension control; 2) diffusion control; and 3) asymmetric distribution. These controls are described in details below explaining our ability to create this complex hybrid pattern.

The ability to control the distribution in three dimensions is an extension of two dimensional control with the streams intersecting in both vertical and horizontal configurations. Three-dimensional control first was analyzed in the 6-inlet vertically-aligned device at location *m*. Cascade blue was added into inlets iii and iv, and PBS into inlets i, ii, v and vi. The solutions in all six inlets were added with equal pressure (approximately 1 psi). From the device configuration, the intersection of the top channels was close to their convergence point with the bottom channels; the liquids did not have time to mix between the top and bottom inlets before reaching this convergence point. Figure 2c is a schematic of the expected distribution pattern near the intersection of the streams at location *m* in Figure 1a. By adjusting the focus plane

on the microscope and using a high numerical aperture objective (1.0, 40X) slices at specific positions in the x-z plane were observed. On the lower layer (at cross-section **l**), 75% of the normalized fluorescence intensity occurred from 0 to 40 μm (in the y-axis) and decreased to 0% from 60 to 100 μm (Fig. 2d). The reverse was observed for the upper layer (at cross-section **u**) with 75% of the normalized intensity occurring between 60 to 100 μm. Hence, cross-section analysis at location *m*, where the inlets converged into the main channel, revealed that three-dimensional distribution exhibited a discrete on-off binary signal that correlated to the presence or absence of fluorescent signal. This device can be used as an extension of a two-dimensional technique for subcellular stimulation for three-dimensional stimulation. By having the ability to control the location and profile in 3 dimensions, a cell can be exposed with separation in the horizontal and vertical directions through the stream interface. Based upon the dimensions of the microfluidics device as well as the width and height of the attached cell, the fluid could flow around the periphery of the cell membrane and not solely over the top of the cell in streamlines; this would create the separation in the vertical direction.

The ability to control a chemical profile depends on the effects of diffusion over the length of the main channel. Hence, diffusion control would allow us to create either a step or sloping chemical gradient. A step gradient, or digital signal profile, resulted from the presence or absence of a chemical, as a discrete on-off binary signal; whereas, a sloping gradient, or analog signal profile, had no abrupt transitions and resulted from a gradual chemical distribution from high to low concentration across the channel. To determine the effect of diffusion over the length of the main channel, the chemical distribution was analyzed at two different locations approximately 3 cm apart (locations *m* and *o* in Fig. 1a). Cascade blue was added into inlets v and vi and PBS into the remainder of the inlets of a 6-inlet vertically-aligned device. Analysis of fluorescence intensity at location *m* showed a step gradient profile (Fig. 3a), whereas examining the chemical distribution at location *o* revealed a sloping gradient (Fig. 3b). Hence, the role of chemical diffusion was observed 3 cm away from the converging point as the step gradient gradually becomes a sloping gradient. We expect a homogeneous (no gradient) chemical distribution to occur in the main channel at a distance further downstream from location *o*. Finally, although our results demonstrated that diffusion occurs in the x-y plane, diffusion between adjacent streams was similar in the x-z plane.

A gradient profile was actively controlled by the amount of diffusion between adjacent lanes, which in turn was actively manipulated by changes in distance and time that the streams were in contact, by the chemical diffusion coefficient, as well as by the flow velocity. As our results indicated, at smaller distances travelled and shorter periods of time where the chemicals were in contact with each other, the amount of diffusion was smaller (Fig. 3a). Conversely, with longer distances and time that the streams ran parallel to each other, the amount of diffusion was greater (Fig. 3b); small molecules such as fluorescein have a diffusion coefficient of 300 $\mu m^2/s$. Through actively controlling the fluid velocity, we dictated the distribution patterns along the main channel in three dimensions. The pressure was associated with the fluid flow speed, which controlled the gradient profile along the main channel length. By increasing the flow rates, the diffusion region was minimized over the length of the main channel, which created a step gradient. The flow velocity of adjacent streams was regulated by adjusting the inlet pressure. Hence, by regulating the initial inlet pressure we controlled fluid flow. As the chemical agents diffused across the interface, the solubilized molecules continued to propagate down length of the main channel (x-axis). The fluorescent intensity gradually decreased across the width (y-axis). Thus a step gradient was actively manipulated by changes in this pressure, distance, and time. For intermediate flow velocities and selected diffusion coefficients, the intensity distribution began as a step gradient at the intersection of the streams in the main channel, but gradually evolved into a sloping gradient at two to three centimetres away from the converging point (Fig. 3b). This pattern had a gradual slope with a maximum intensity at the right edge (100 micrometers) of the cross-section and a minimum intensity at the opposite end (0 micrometers). The gradients shown can create patterns that are not solely binary in both 2 and 3 dimensions. While we demonstrated this for a simple 3 lane system, more complex distributions can be developed easily through implementing a multitude of inlets converging at a central channel.

The gradient profile was actively controlled because decreasing the flow velocity increased the amount of diffusion between the streams at a distance further along the main channel relative to the initial channel intersection.

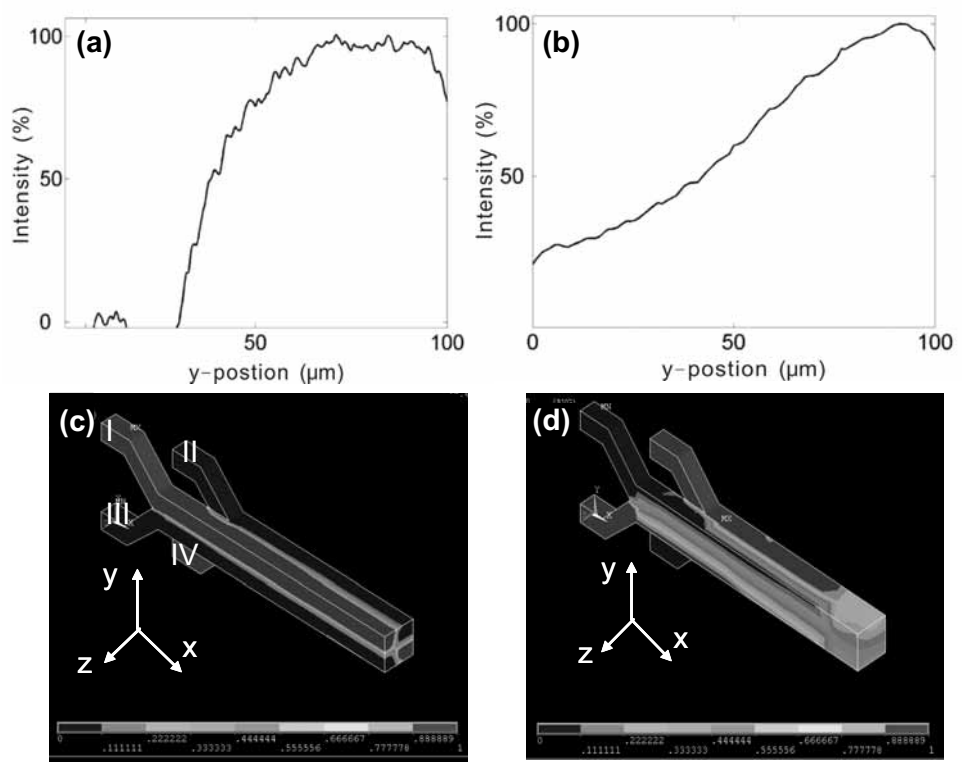

Figure 3 : Diffusion control for fluid molecular gradient patterns in MuFS-3D. (a) Distribution for a 6-inlet vertically-aligned device with cascade blue in PBS in lanes v and vi with the remainder of the lanes with PBS. Normalized intensity plot of the cross-section in the fluidics system for location *m* in Figure 1 revealing a discrete step gradient. (b) Normalized intensity plot across the cross-section with a continuous sloping gradient at location *o* for the same conditions as (a) revealing the same main channel having both step and sloping gradients. (c) Analysis of pressure control using ANSYS 4-inlet vertically-offset models. A solution with chemical dye (red) was inserted into inlets I and IV whereas a control solution (blue) was inserted into inlets II and III. The chemical distribution pattern when an inlet pressure of 3 psi was used. A high inlet pressure resulted in a distinct step gradient along the length of the main channel. (d) The chemical distribution pattern when an inlet pressure of 0.1 psi was used. Shortly after the streams converged, the gradient became sloped with significant mixing. The color bars indicate levels of chemical concentration in the channels with no molecules present at the left side of the bar (blue end) to complete molecular presence on the right side of the bar (red end).

Therefore, two profiles were observed: 1) a digital signal profile, or step gradient, due to the presence or absence of a chemical; 2) an analogue system, or sloping gradient, where the distributions were gradually sloped gradients of chemicals across the cross-sections due to increasing the time of interface interaction.Analogue signals in the electronic media world vary continuously with time and have no abrupt transitions between levels, while digital system are discretized into sequences of binary, on-or-off representations. We have shown the ability to create these patterns and we actively manipulate them using aqueous media.

Computational simulation of a three-dimensional flow pattern in a 4-inlet vertically-offset device was created using ANSYS (Figs. 3c and 3d). The computational simulation was completed with the dimensions matching those used in our experimental system. The fluid flow and diffusion effects were modeled by FLOTRAN CFD with the multi species function in ANSYS. Within the model, a solution containing a chemical dye was inserted into inlets I and IV whereas a control solution was inserted into inlets II and III. The lack or presence of chemical dye was color labelled as a blue or red solution, respectively. In the ANSYS model, momentum

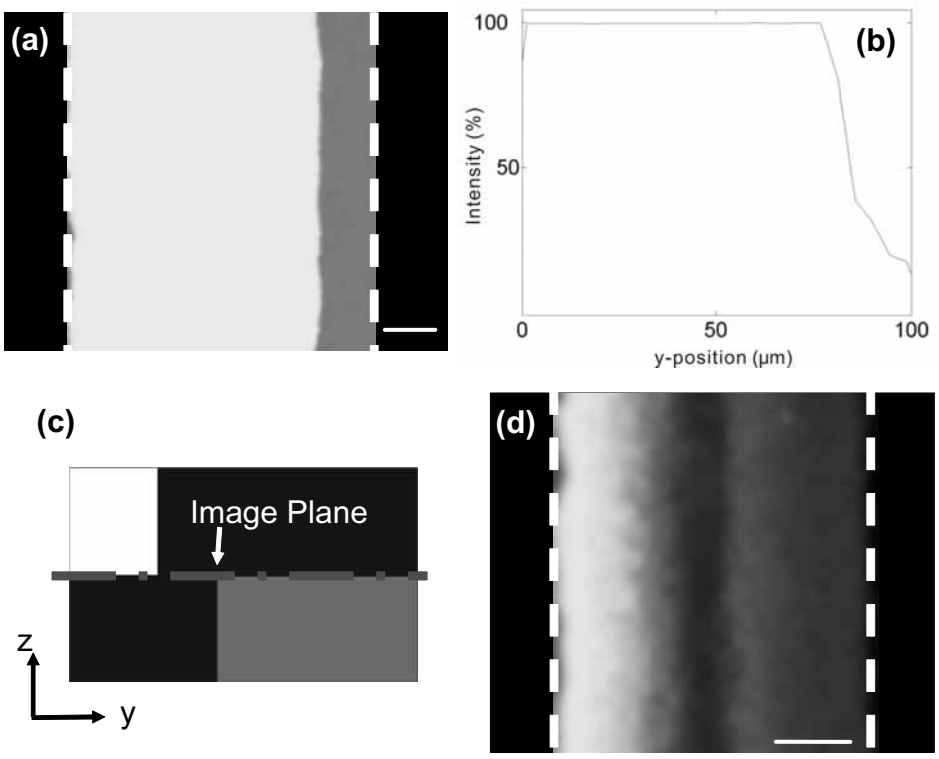

Figure 4 : Control of asymmetric molecular pattern formation by pressure differentials and flow velocities. (a) Fluorescence micrograph and (b) normalized intensity plot of a 6-inlet vertically-aligned device at location *m*. Fluorescein was added into inlets i, ii, iv and v and texas red into inlets iii and vi. An asymmetric chemical distribution was observed as the pressure for fluorescein was increased compared to texas red. Scale bar = 15 μm. (c) Schematic of distribution of fluorescence with unequal amounts of fluorescein in inlet i and cascade blue in inlet v and vi along with higher pressures of PBS in ii and iii and a lower pressure of PBS in inlet vi from Figure 1. (d) Confocal microscopy image at the image plane labelled in (c). These images were digitally deconvolved and dashed lines in the images indicate the boundaries of the channel. Scale bar =25μm.

equations for the flow field as well as the transport equations were solved for the chemical distribution (Figs. 3c and 3d). By controlling the inlet pressure in the model, three-dimensional phase separation in the main channel was controlled; for the model shown in Figure 3c, an inlet pressure of 3 psi was used. This high inlet pressure resulted in a very distinct step gradient not only at the intersection point but further down the length of the main channel. For the model in Figure 3d an inlet pressure of 0.1 psi was used. For this configuration, the free interface between the streams was a major focus. The stream-wall interface would have a pronounced effect near the wall; this is limited for our system. As we approach the stream-wall interface, additional complex distributions would occur. Although a small initial step gradient was present, the gradient became sloped shortly down the length of the main channel, where significant fluid mixing was observed. Hence, the ANSYS models indicated that by actively manipulating the inlet pressure in our MuFS-3D device we achieved active three-dimensional control of chemical delivery.

As a final mode of control, we imposed a pressure differential that resulted in asymmetric patterns in three dimensions. Equalizing the parameters for all of the inlets allowed us to create symmetrically distributed patterns that were similar to digital and analogue signals. Pressure differentials, from 0.1 to 3 psi, provided the capacity for the control of step and sloping chemical gradients as well as inhomogeneous distribution. By independently changing the inlet pressure in each of the fluidic channels we actively controlled the distribution of the fluids in the main channel. To analyze the effect of pressure on chemical distribution, fluorescence was analyzed in a 6-inlet

vertically-aligned device at location *m*. Fluorescein was added into inlets i, ii, iv, and v and texas red into inlets iii and vi (Fig. 4a). We created much smaller width distribution of the fluorescent molecules (around 10μm) across the 100μm cross-section of the channel through these differential pressures. The profile of the fluids in the main channel was actively shifted through the addition or subtraction of liquid at the inlet as a function of both vertical and horizontal positions. In the 6-inlet vertically-aligned configuration, the increase in the pressure in inlet i and ii relative to inlet iii created a subsequent decrease in the width of one stream (Fig. 4b). The streams were also modulated in the z-axis through differential amounts of liquid introduced into channels above one another on the same side of the main channel. This allowed us to have three-dimensional control of this asymmetric pattern formation shown in the schematic in Figure 4c and a microscopic image at the midplane of the main channel (Fig. 4d). An advantage of our system resulted from the ability to actively manipulate differential pressures which enabled us to create very narrow chemical streams (down to single micrometers in width). Hence, by regulating the initial pressure we control chemical distribution.

Three-dimensional control resulted not only from the choice of inlet but also by modifying the point of entry of the inlet streams into the main channel. In our MuFS-3D vertically-offset device, inlet streams on the upper layer converged into the main channel hundreds of micrometers before the convergence of the inlet streams from the lower layer. This allowed for a gradient profile on the upper layer where diffusion played a more significant role, while simultaneously having little or no diffusion on the lower layer. Furthermore, the distribution of the streams was controlled by having different pressures into each inlet to create a biasing in the chemical distributions. Combining these together, the pattern was a complex hybrid cross section of the main channel and actively controlled using our MUFS-3D device as observed in Figure 2b. Thus, our results have shown our ability to create complex chemical distribution patterns using our MuFS-3D device by actively controlling three-dimensional chemical delivery, the rate of diffusion as well as by asymmetric distribution based on pressure control.

MuFS-3D enabled us to create multiphase molecular three-dimensional aqueous pattern formation using a simple lithographically constructed system. Our results illustrate that we actively control laminar flow in time and space inside the channel. This results in multivariable controls including dimensional positioning of molecular profiles and allows us to be able to parallel digital and analogue signals with aqueous media. With this technique, we precisely manipulate distinct spatial regions of a single main channel by delivering different fluids into selected areas for potential use in numerous applications including three-dimensional chemical fabrication. Furthermore, by integrating our technique with cellular studies, it is possible to chemically stimulate and manipulate subcellular domains of single cells in three dimensions. This potentially can address localized questions in cellular research including structural manipulation of cells where controlled delivery of cytoskeletal disruptors such as latrunculin could be targeted to local domains of cells to determine the effects of three-dimensional separated actin depolymerization. Thus, our MuFS-3D device provides a novel system for studying novel scientific questions in a range of diverse fields including biology, chemistry, physics, and engineering.

Acknowledgement: The authors would like to thank G. Fedder in the Department of Electrical and Computer Engineering at Carnegie Mellon University and the Center of Biologic Imaging Lab at the University of Pittsburgh. The authors also acknowledge A. Antúnez de Mayolo, F. Higgs, W. Messner, and A. Tsourkas for valuable discussions about this research and comments on the manuscript. This work was supported in part by the National Science Foundation-CAREER, Pennsylvania Infrastructure Technology Alliance, and the Department of Energy-Genome to Life.

References

1. Groisman, A., Enzelberger, M., & Quake, S. R. (2003) *Science* **300**, 955-958.

2. Takayama, S., Ostuni, E., LeDuc, P., Naruse, K., Ingber, D. E., & Whitesides, G. M. (2001) *Nature* **411**, 1016.

3. Takayama, S., Ostuni, E., LeDuc, P., Naruse, K., Ingber, D. E., & Whitesides, G. M. (2003) *Chem. Biol.* **10**, 123-130.

4. Foster, K., & Parker, G. A. (1970) *Fluidics, Components and Circuits* (Wiley-Interscience, London).

5. Humphrey, E. F., & Turamoto, D. H. (1965) *Fluidics, Fluid Amplifier Associates* (Boston, MA).

6. Ismagilov, R. F., Ng, J. M. K., Kenis, P. J. A., & Whitesides, G. M. (2001) *Anal. Chem.* **73**, 5207-5213.

7. Chung, S., Im, Y., Choi, J., & Jeong, H. (2004) *Microelectro. Eng.* **75**, 194-200.

8. Yang, H. K., Kim, M. S., Kang, S. W., Kim, K. S., Lee, K. S., Park, S. H., Yang, D. Y., Kong, H. J., Sun, H. B., Kawata, S., & Fleitz, P. (2004) *J. Photopolymer Sci. Tech.* **17**, 385-392.

9. Verpoorte, E., & De Rooij, N. F. (2003) *Proc. IEEE* **91**, 930-953.

10. Shoji, S., & Esashi, M. (1993) *Appl. Biochem. Biotechnol.* **41**, 21-34.

11. Voldman, J., Gray, M. L., & Schmidt, M. A. (1999) *Annu. Rev. Biomed. Eng.* **1**, 401-425.

12. Deisingh, A. K. (2003) *Analyst* **128**, 9-11.

13. Madou, M. J. (2002) *Fundamentals of Microfabrication, Vol. Second Edition* (CRC Press, New York, NY).

14. Xia, Y., Kim, E., Zhao, X. M., Rogers, J. A., Prentiss, M., & Whitesides, G. M. (1996) *Science* **273**, 347-349.

15. Xia, Y., Rogers, J. A., Paul, K. E., & Whitesides, G. M. (1999) *Chem. Rev.* **99**, 1823-1848.

16. Kenis, P. J., Ismagilov, R. F., & Whitesides, G. M. (1999) *Science* **285**, 83-85.

17. MacDonald, M. P., Paterson, L., Volke-Sepulveda, K., Arlt, J., Sibbett, W., & Dholakia, K. (2002) *Science* **296**, 1101-1103.

18. MacDonald, M. P., Spalding, G. C., Dholakia, K. (2003) *Nature* **426**, 421-424.

19. Chiu, D. T., Pezzoli, E., Wu, H., Stroock, A. D., & Whitesides, G. M. (2001) *Proc. Natl. Acad. Sci. USA* **98**, 2961-2966.

20. Koo, J. M., & Kleinstreuer, C. (2003) *J. Micromech. Microeng.* **13**, 568-579.

21. Moore, S. K. (2001) *IEEE Spectrum* **38**, 28-29.

22. Terray, A., Oakey, J., & Marr, D. W. (2002) *Science* **296**, 1841-1844.

23. Kirk, J. S., & Bohn, P. W. (2004) *J. Am. Chem. Soc.* **126**, 5920-5926.

24. Shen, F., Poncet-Legrand, C., Somers, S., Slade, A., Yip, C., Duft, A. M., Winnik, F. M., & Chang, P. L. (2003) *Biotechnol. Bioeng.* **83**, 282-292.

25. Yi, G. R., Thorsen, T., Manoharan, V. N., Hwang, M. J., Jeon, S. J., Pine, D. J., Quake, S. R., & Yang, S. M. (2003) *Adv. Mat.* **15**, 1300-1304.

26. Beebe, D. J., Moore, J. S., Yu, Q., Liu, R. H., Kraft, M. L., Jo, B. H., & Devadoss, C. (2000) *Proc. Natl. Acad. Sci. USA* **97**, 13488-13493.

27. Jo, B. H., Van Lerberghe, L. M., Motsegood, K. M., & Beebe, D. J. (2000) *J. Microelectromech. Syst.* **9**, 76-81.

28. Roulet, J. C., Volkel, R., Herzig, H. P., Verpoorte, E., de Rooij, N. F., & Dandliker, R. (2001) *J. Microelectromech. Syst.* **10**, 482-491.

29. Sundararajan, N., Pio, M. S., Lee, L. P., & Berlin, A. A. (2004) *J. Microelectromech. Syst.* **13**, 559-567.

30. White, F. M. (1986) *Fluid mechanics, second edition* (McGraw-Hill, Inc., New York).